The *extended auricle1* (*eta1*) Gene Is Essential for the Genetic Network Controlling Postinitiation Maize Leaf Development

Karen S. Osmont, Lynne A. Jesaitis[1] and Michael Freeling[2]

Department of Plant and Microbial Biology, University of California, Berkeley, California 94720

Manuscript received April 8, 2003
Accepted for publication July 11, 2003

ABSTRACT

The maize leaf is composed of distinct regions with clear morphological boundaries. The ligule and auricle mark the boundary between distal blade and proximal sheath and are amenable to genetic study due to the array of mutants that affect their formation without severely affecting viability. Herein, we describe the novel maize gene *extended auricle1* (*eta1*), which is essential for proper formation of the blade/sheath boundary. Homozygous *eta1* individuals have a wavy overgrowth of auricle tissue and the blade/sheath boundary is diffuse. Double-mutant combinations of *eta1* with genes in the *knox* and *liguleless* pathways result in synergistic and, in some cases, dosage-dependent interactions. While the phenotype of *eta1* mutant individuals resembles that of dominant *knox* overexpression phenotypes, *eta1* mutant leaves do not ectopically express *knox* genes. In addition, *eta1* interacts synergistically with *lg1* and *lg2*, but does not directly affect the transcription of either gene in leaf primordia. We present evidence based on genetic and molecular analyses that *eta1* provides a downstream link between the *knox* and *liguleless* pathways.

IN plants, lateral organs such as leaves are born on the flanks of meristems (Steeves and Sussex 1989). This is a reiterative process, which originates with recruitment of segment initial cells to form a phytomer composed of leaf, node, internode, and axillary bud (Scanlon *et al.* 1996). A subset of these cells initiates the leaf and is termed the leaf founder cells (Poethig 1984). These founder cells divide, giving rise to leaf primordia, which undergo longitudinal differentiation that occurs basipetally (from tip to base such that blade differentiates prior to sheath) as well as laterally from the midrib to the margin (Harper and Freeling 1996b). The maize leaf provides a simple model for examining the genetic cues involved in organ regional identity and cell fate determination.

The ligule, a morphological feature of the grasses, is an epidermal fringe of tissue derived from the adaxial leaf surface. The ligule bisects the longitudinal, or proximodistal, axis of the leaf into proximal sheath and distal blade (Figure 1). Along with the ligule, a pair of triangular-shaped auricles forms the blade/sheath boundary. Differentiation of auricle is first visible as a thin line of cells that separates the blade and sheath, which can be seen only after initiation of the ligule (Becraft *et al.* 1990). The auricle cells enlarge concomitantly with ligule outgrowth and then divide as the blade and sheath expand. After the leaf emerges, the auricle cells expand further, allowing the leaf blade to bend out horizontally from the main axis.

Our understanding of ligule and auricle development stems from analysis of leaf structures in wild-type plants as well as in mutant plants that show disruptions at the blade/sheath boundary. Aberrations in the auricle are often associated with a disrupted ligule, implying that their development is closely linked. Mutants that affect the auricle and/or the blade/sheath boundary include *lg1, lg2, rs2, Rs1, Lg3, Kn1*, and *Gn1* (see below and Table 1). These mutants can be divided into two distinct groups. The first group is defined by recessive mutants that show altered ligule and auricle development resulting from absence of essential proteins during leaf primordial development. The second group is defined by mutants that affect proximodistal identity and ectopically express KNOX proteins in the leaf.

The first group of genes consists of *liguleless* (*lg1*) and *liguleless2* (*lg2*). Recessive mutants of *lg1* remove both the ligule and auricle, but a rudimentary ligule is formed in the upper leaves (Becraft *et al.* 1990; Sylvester *et al.* 1990). Recessive mutants of *lg2* remove the ligule and auricle in the first one to three leaves. The ligule and auricle recover in later leaves but the blade/sheath boundary remains displaced. Double-mutant analysis of *lg1* and *lg2* revealed that these two genes interact in a dosage-dependent manner (Harper and Freeling 1996a). Double-mutant *lg1 lg2* plants fail to form a ligule or auricle and the blade/sheath boundary is diffuse (Harper and Freeling 1996a). Reverse transcriptase (RT)-PCR analysis showed that LG2 expression precedes that of LG1 (Walsh *et al.* 1998). These genetic and molecular analyses have shown that *lg1* and *lg2* act

[1]*Present address:* Pointilliste, 2541 Leghorn St., Suite 4, Mountain View, CA 94043.

[2]*Corresponding author:* Department of Plant and Microbial Biology, University of California, 111 Koshland Hall, Berkeley, CA 94720. E-mail: freeling@nature.berkeley.edu

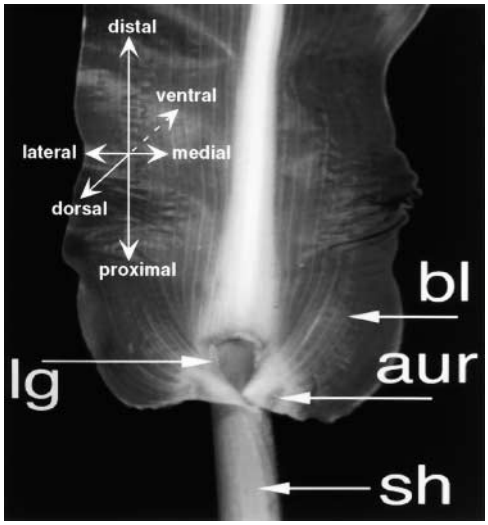

FIGURE 1.—A typical maize leaf can be divided along three axes, the proximodistal, mediolateral, and dorsiventral or ad/abaxial. Auricle (aur) and ligule (lg) mark the proximodistal boundary between proximal sheath (sh) and distal blade (bl).

in the same genetic network late in leaf development to induce ligule and auricle formation (HARPER and FREELING 1996a; WALSH *et al.* 1998). Both *lg1* and *lg2* have been cloned and encode nuclear-localized proteins with homology to squamosa promoter binding proteins and bZIP transcription factors, respectively (MORENO *et al.* 1997; WALSH *et al.* 1998).

The second group of genes affecting the blade/sheath boundary includes mutants that ectopically express KNOX proteins in the leaf, resulting in alteration of regional identity and formation of proximal tissues more distally (*i.e.*, the sheath forms or extends into the leaf blade; FREELING 1992; MUEHLBAUER *et al.* 1997). The *knotted1* (*kn1*) gene was first defined by dominant alleles that cause formation of knots over lateral veins and ectopic ligule in the blade (FREELING and HAKE 1985), and the mutant phenotype was found to be caused by ectopic expression of *kn1*, a homeobox gene, in the leaves (HAKE *et al.* 1989; VOLLBRECHT *et al.* 1991). The class 1 *knotted1-like homeobox* (*knox*) genes *rough sheath1* (*rs1*), *gnarley1* (*gn1*), and *liguleless3* (*lg3*) have also been defined by dominant mutants (BECRAFT and FREELING 1994; FOWLER and FREELING 1996; KERSTETTER *et al.* 1997; FOSTER *et al.* 1999). On the basis of loss-of-function phenotypes, the *knox* genes are thought to be required for meristem maintenance and to repress differentiation, although the precise function of these genes has not been determined (KERSTETTER *et al.* 1997; VOLLBRECHT *et al.* 2000). In Arabidopsis, the *knox* genes *SHOOT MERISTEMLESS* (*STM*) and *KNAT1* (*KNOTTED1-LIKE IN ARABIDOPSIS THALIANA*) may act redundantly to confer meristematic identity (LONG *et al.* 1996; BYRNE *et al.* 2002).

Another member of the second group has been defined by recessive mutants in *rough sheath 2* (*rs2*). Mutants of *rs2* have several phenotypic effects, including dwarfing, disruption of the blade sheath boundary, twisting of the leaves, loss of blade tissue, and disorganization of cell division resulting in leaf proximalization (SCHNEEBERGER *et al.* 1998). RS2 encodes a MYB-domain-containing factor with homology to the *PHANTASICA* (*PHAN*) gene from Antirrhinum and the *ASYMMETRIC LEAVES1* (*AS1*) gene from Arabidopsis (TIMMERMANS *et al.* 1999; TSIANTIS *et al.* 1999; BYRNE *et al.* 2000; ORI *et al.* 2000). *AS1* is required for suppression of the Arabidopsis *KNOX* genes *KNAT1*, *KNAT2*, and *KNAT6* in the leaf (ORI *et al.* 2000). Genetic evidence suggests that *STM* acts to suppress *AS1* and *AS2* in the meristem to prevent initiation of the leaf developmental program (BYRNE *et al.* 2000, 2002). In addition, the *PICKLE* (*PKL*) gene, which encodes a chromatin-remodeling factor of the CHD class, enhances *as1* and *as2* mutants, indicating that *PKL* may have a general role in repression of *KNOX* genes in the leaf via changes in chromatin structure (ORI *et al.* 2000). Expression studies of *rs2* mutants revealed the *knox* genes *lg3, kn1*, and *rs1* are ectopically expressed in the leaf (SCHNEEBERGER *et al.* 1998). The *rs2* gene is normally expressed in leaves whereas *knox* genes are expressed in the shoot apical meristem (TIMMERMANS *et al.* 1999; TSIANTIS *et al.* 1999). These molecular and

TABLE 1

Alleles used in this study

Allele	Dominance	Protein homologies	Phenotypes	Reference
lg1-R	Recessive	Squamosa-like BP	Absence of ligule, auricle	MORENO *et al.* (1997)
lg2-219	Recessive	bZIP TF	Absence of ligule, auricle in lower leaves	WALSH *et al.* (1998)
Kn1-N	Semidominant	Class 1 *knox* TF	Ectopic knots, ligule prominent venation	VOLLBRECHT *et al.* (1991)
Rs1-O	Dominant	Class 1 *knox* TF	Rough sheath, proximalization	SCHNEEBERGER *et al.* (1995)
Gn1-R	Dominant	Class 1 *knox* TF	Altered ligule, sheath	FOSTER *et al.* (1999)
Lg3-O	Semidominant	Class 1 *knox* TF	Blade to sheath transformation	MUEHLBAUER *et al.* (1997)
rs2-R	Recessive	Myb-like TF	Rough sheath, proximalization	SCHNEEBERGER *et al.* (1998)
eta1-R	Recessive	Unknown	Extended auricle	This study

genetic data suggest that the RS2/AS1/PHAN protein family functions to repress *knox* genes in the leaf.

Other components of the *knox* gene pathway include the maize mutant *semaphore1* (*sem1*). *sem1* acts to repress a subset of the *knox* genes in the maize leaf, mainly the genomic duplicates *gn1* and *rs1* (Scanlon *et al.* 2002). KNOX proteins appear to function through interactions with the BEL1 class of homeodomain proteins in both monocots and dicots (Bellaoui *et al.* 2001; Mueller *et al.* 2001; Smith *et al.* 2002). Plant growth hormones are also regulated by *knox* gene action. KNOX proteins inhibit the expression of GA 20-oxidase in tobacco, tomato, and Arabidopsis, presumably inhibiting GA biosynthesis, while overexpression of *knotted1* causes increased levels of cytokinin in tobacco (Li *et al.* 1992; Ori *et al.* 1999; Sakamoto *et al.* 2001; Hay *et al.* 2002).

We have identified a novel maize gene called *extended auricle1* (*eta1*) on the basis of the behavior of a recessive mutant allele. Homozygous *eta1* individuals have a wavy overgrowth of auricle tissue and the blade/sheath boundary is diffuse. However, one or two doses of *eta1* mutant alleles result in synergism and enhancement of *liguleless* and *knox* phenotypes. We provide evidence based on genetic and molecular analyses with *eta1* that the *knox* and *liguleless* pathways are linked in the genetic network controlling maize leaf development. These data also suggest that *eta1* may function downstream of these pathways and show it is a key player in maize leaf development.

MATERIALS AND METHODS

Origin of the *eta1-R* allele: The *eta1* reference allele, *eta1-R*, originated from an EMS screen of M2 segregating families performed by the Hollick lab (UC-Berkeley).

Mapping and introgression: The *eta1-R* mutation was introgressed five to seven times into the inbred lines Mo17, B73, W22, W23, and A188 via backcrossing and self-pollination. Individuals homozygous for *eta1-R* were pollinated by B-A translocation stocks for mapping (Beckett 1994a). Resultant F_1 individuals were planted, scored, and compared to segregating *eta1-R* families derived from the same parental *eta1-R* plants. Families segregating *eta1-R* were outcrossed to the inbred lines Mo17, B73, and W22 and then self-pollinated. The subsequent F_2 families were used for fine mapping with simple sequence repeats (SSRs) and restriction fragment length polymorphisms (RFLPs).

Double-mutant stocks: Sarah Hake kindly provided *Kn1-N* and *Gn1-R* in the W22 background. Heterozygous *Kn1-N* and *Gn1-R* individuals were crossed to homozygous *eta1-R* individuals in the W22 background. F_1 individuals displaying the *Kn1-N* or *Gn1-R* phenotypes were backcrossed to *eta1-R* homozygotes in the case of *Kn1-N* or self-pollinated in the case of *Gn1-R*. The spontaneous *lg1-R* mutation was originally obtained from the Maize Genetics Stock Center (Urbana, IL) and backcrossed six generations into the Mo17 background. The *lg1-R* mutation was crossed to *eta1-R* in the Mo17 background. The *lg2-219* allele was isolated in a directed *Mutator*-tagging experiment (Walsh *et al.* 1998) and was backcrossed into the inbred line W23 for three generations. Homozygous *lg2-219* individuals were crossed to *eta1-R* homozygotes in the W22 and Mo17 backgrounds. The dominant dosage effect of *eta1-R* heterozygotes with *lg2-219* was seen in all double-mutant families independent of background. The genotypes of individuals displaying the *eta1-R/+ lg2-219/lg2-219* dosage phenotype were determined with the SSR marker linked to *eta1-R*. They were also test crossed to the *eta1-R* single mutant to confirm the dosage effect. The *rs2-R* allele was obtained from the Maize Genetics Stock Center and backcrossed into the inbred line Mo17 for five generations. Homozygous *eta1-R* individuals in the Mo17 background were crossed to *lg1-R* and *rs2-R* homozygotes in the Mo17 background. The resultant F_1 individuals were self-pollinated and scored in the F_2 generation. The *Lg3-O* and *Rs1-O* alleles were obtained from the Maize Genetics Stock Center and backcrossed for seven generations into the Mo17 background. Individuals heterozygous for either *Lg3-O* or *Rs1-O* were crossed to *eta1-R* homozygous individuals in the Mo17 background. The resultant F_1 individuals were either self-pollinated in the case of *Rs1-0* or outcrossed to *eta1-R* homozygotes in the case of *Lg3-O* (see Table 2).

PCR: DNA was isolated for PCR using the method described previously (Edwards *et al.* 1991). The primers umc1221 forward and reverse were used to amplify the SSR linked to *eta1-R* (umc1221 forward, GCAACAGCAACTGGCAACAG; umc1221 reverse, AAACAGGCACAAAGCATGGATAG). Additional SSR primers used in mapping included umc1171 forward and reverse, mmc0081 forward and reverse, and umc1060 forward and reverse (for primer sequences and amplification conditions refer to http://www.agron.missouri.edu). The RFLP csu308 was also used in fine mapping the *eta1-R* mutation.

Environmental scanning electron microscope analysis: Seedlings were harvested at 4 weeks from an *eta1-R* segregating family in the W23 background. Fresh leaves were dissected and mounted on metal stubs for imaging with an Electroscan E3 environmental scanning electron microscope (ESEM) located at the Electron Microscope Laboratory (UC-Berkeley).

Reverse transcriptase-PCR gel blot analysis: RNA was isolated from 3-week-old seedlings in *eta1-R* segregating families in the Mo17 and W22 backgrounds. The meristems and p1–5 leaves from three individuals were pooled as were the p6–8 leaves at the ligule ridge stage. RNA isolation was performed using TRIzol (Invitrogen, San Diego). RNA was treated with DNaseI and then reverse transcribed using Superscript II reverse transcriptase (RT) and an oligo(dT) primer (Invitrogen). Gene-specific primers for the *liguleless1*, *ubiquitin* (Moreno *et al.* 1997), *liguleless2* (Walsh *et al.* 1998), *knotted1, gnarley1, roughsheath1, liguleless3, liguleless4a*, and *liguleless4b* genes were used to PCR amplify the corresponding genes from the resulting cDNAs. The PCR reactions were run for 20 cycles. The gene products were detected via Southern blot hybridization with gene-specific probes. RT-PCR was performed on independent RNA pools at least three times for each gene. RT-PCR reactions were repeated with the *knox* gene primers and amplified for 30 cycles to confirm expression patterns in the *eta1-R* segregating families. Primers for the *knox* genes were as follows: kn1-5′, AGCTCGCTCAAGCAA GAACTGTC; kn1-B2, CATAGGCGCATATAGATAGAGTAGC AAC; gn1-B1, TACGCAGAAACACTCCGACACGGTCG; gn1-F2, GGAAGACGACGACATGGATCCGAG; rs1-11464, TTCTGAAG ATGACATGGACCCGAATGGTC; rs1-pbo7, GAGAACTACAA GCCATGCATAGACGCTAC; lg3/4-1, GTGGAACACGCACTAC CGCTG; lg3-D2, TGAGCTGGCCAGTTGTCATCCC; lg4a-B1, CCAGTATGCTGAGTGTACCTACCGACAC; and lg4b-B1, CGA CAATACACGTTGTCGCCCATGC.

Northern blot analysis: RNA was isolated from 3- to 4-week-old seedlings in an *eta1-R Kn1-N*-segregating family in the W22 background. RNA was isolated using the TRIzol method (Invitrogen). Poly(A)$^+$ RNA was then isolated using the oligotex mRNA miniprep kit from QIAGEN (Valencia, CA). Approxi-

TABLE 2

Double-mutant analysis

		Phenotypic classes				
Family	Interaction	wt	*lg1*	*eta1*	*lg1 eta1*	
lg1-R eta1-R[a]	Synergistic	158	75	71	22	
Family	Interaction	wt	*lg2*	*eta1*	*eta1/+ lg2*	*eta1 lg2*
lg2-219 eta1-R[a]	Synergistic	76	13	19	11	8
Family	Interaction	wt	*Kn1*	*eta1*	*Kn1 eta1*	
Kn1-N eta1-R[b]	Enhancement	36	28	34	36	
Family	Interaction	wt	*Rs1*	*eta1*	*Rs1 eta1*	
Rs1-0 eta1-R[a]	Synergistic	29	70	9	25	
Family	Interaction	wt	*Gn1*	*eta1*	*Gn1 eta1*	*Gn1/Gn1 eta1*
Gn1-R eta1-R[a]	Dose-dependent synergistic	25	62	7	14	5
Family	Interaction	wt	*Lg3*	*eta1*	*Lg3 eta1*	
Lg3-0 eta1-R[b]	Enhancement	49	62	42	53	
Family	Interaction	wt	*rs2*	*eta1*	*rs2 eta1*	
rs2-R eta1-R[a]	Synergistic	366	98	133	44	

[a] Segregating families resulted from a self-pollination event of an F_1 individual heterozygous for both alleles.
[b] Segregating families resulted from an outcross of heterozygous F_1 individuals to individuals homozygous for the *eta1-R* allele.

mately 2 μg poly(A)$^+$ RNA was loaded on a formaldehyde-containing 1% agarose gel and subjected to gel electrophoresis at 72 V for 2.5 hr. The RNA was transferred for 4 hr to nylon membrane (Hybond-NX). Membranes were hybridized in 1 M sodium phosphate buffer, pH 7.2, 7% SDS, and 1 mM EDTA. A *kn1* cDNA probe obtained from the Hake lab was used for hybridization (Smith *et al.* 1992). An *ubiqitin* probe was used as a loading control.

RESULTS

Phenotypic analysis and effect of genetic background on *eta1*: The *eta1-R* mutation was originally isolated from an EMS mutagenesis screen. The *eta1* phenotype segregates as a single recessive locus in F_2 families. The most notable phenotype of *eta1* is an overgrowth or extension of auricle tissue. The *eta1* mutant is pleiotropic and displays a range of phenotypes, including displacement of the blade/sheath boundary, disruption of the ligule, reduction in internode spacing and overall plant height, and the production of smaller, more compact ear shoots (Figure 2, A–D).

To determine the developmental basis of the *eta1* phenotype, ESEM analysis was used to compare wild-type and *eta1* siblings (Figure 2, E–H). The blade/sheath boundary of *eta1* mutants is severely displaced relative to wild type (Figure 2, E *vs.* F). The blade/sheath boundary normally runs perpendicular to the proximodistal axis of the leaf, thus forming a boundary between blade and sheath. However, the blade/sheath boundary of *eta1* individuals runs nearly parallel to the proximodistal leaf axis (Figure 2F). In addition, the ligule fails to form completely in *eta1* mutants. Although somewhat disorganized, morphologically recognizable blade, sheath, ligule, and auricle cells are visible in *eta1* individuals. Examination of the auricle cells in *eta1* mutants reveals some aberrant, disorganized divisions, but the auricle cell shape and size are comparable to those of wild type (Figure 2, G and H).

Given the pleiotropic nature of the *eta1-R* allele, it was introgressed into five different maize inbred lines to determine the most expressive phenotypes and to help elucidate a precise *eta1* function. As with many maize developmental mutants, *eta1* displays background effects, but is fully penetrant in all inbred lines tested. Background effects have been previously documented with maize heterochronic mutants as well as with dominant *knox* mutants (Poethig 1988; Fowler and Freeling 1996). The auricle phenotype is most severe in Mo17 and W23, in which the auricles become highly elaborated, sometimes even forming a collar-like struc-

ture similar to the morphology of the blade/sheath boundary of rice (Figure 3A). The auricle phenotype is least severe in B73 with auricle extension only along the margin in adult leaves and little to no auricle extension in juvenile leaves (Figure 3B). In all of the genetic backgrounds tested, *eta1* mutant plant height compared to wild-type siblings was similarly reduced (see Table 3). The most penetrant *eta1* phenotypes were the reduction in plant height and the displacement of the blade sheath boundary, which enabled consistent scoring even in weakly expressing backgrounds.

Mapping and dosage: The *eta1* mutation was initially mapped using B-A translocation stocks, using standard procedures (Beckett 1994b). The translocation 5Ld uncovered the *eta1* phenotype, indicating that the *eta1* locus is distal to this chromosome breakpoint on the long arm of chromosome 5. The phenotype of *eta1-R* hemizygotes is equivalent to *eta1-R* homozygotes, suggesting that the *eta1-R* allele is an amorph or has complete loss of function. SSR markers (Smith *et al.* 1997) were then used to fine map *eta1*. Linkage was first found to the marker mmc0081, which maps to bin 5.05 (bin number is a positional designation along maize chromosomes; for example, chromosome 5 is divided into nine bins). SSRs in bins 5.04 and 5.05 were then tested for linkage. The SSR umc1221 located at position 329.5 in bin 5.04 was found to be closely linked to *eta1* at a recombination distance of 1 cM. This marker was subsequently used for determination of *eta1* genotype.

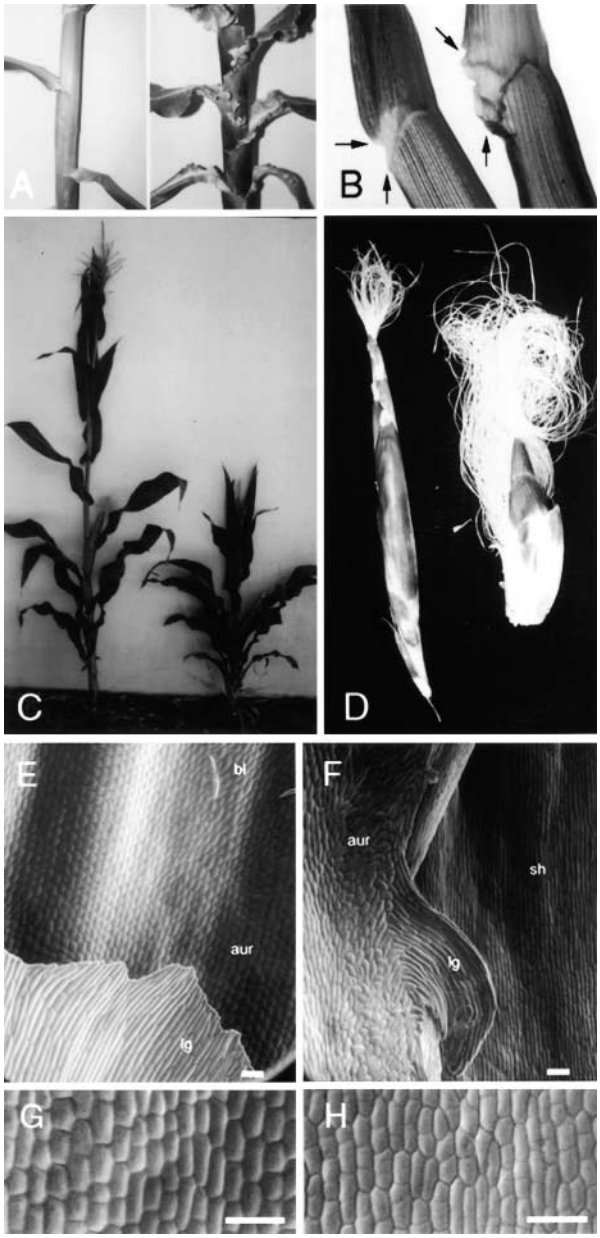

Figure 2.—Pleiotropic effects of the *eta1-R* mutation. (A) Mo17 siblings in an *eta1-R*-segregating family, wild type on the left and *eta1* on the right. Note the compaction of internodes and auricle extension. (B) W22 siblings in an *eta1-R*-segregating family, wild-type leaf on the left and *eta1* on the right. Note the displacement of the blade/sheath boundary and the interrupted ligule line. Extension of auricle can be seen as lighter tissue extending up into the darker green blade. Arrows mark the auricle tissue in wild type and *eta1*. (C) A188 siblings in an *eta1-R*-segregating family, wild type on the left and *eta1* on the right. Plant height is reduced to approximately one-half of wild type. (D) Ear shoots of an *eta1-R*-segregating family in the Mo17 background, wild-type ear on the left and *eta1* mutant ear on the right. The *eta1* ear is more compact and husk leaves fail to form completely around the developing ear shoot. (E–H) ESEM images of the adaxial leaf surface of wild-type and *eta1* individuals in a W23 background. The leaves imaged here are just extruding from the whorl, are the sixth leaf produced, and are approximately plastochron 10. (E) Wild-type leaf at the blade/sheath boundary. (F) *eta1* leaf at the blade/sheath boundary. (G) Wild-type auricle cells. (H) *eta1* auricle cells. Lg, ligule; sh, sheath; aur, auricle; bl, blade. Bar, 50 μm.

Double-mutant analysis

***eta1* interacts synergistically with the *liguleless1/liguleless2* pathway:** Both the *lg1* and *lg2* genes function in formation of the blade/sheath boundary and elaboration of ligule and auricle. Mutants of *lg1* and *lg2* show a dosage-dependent genetic interaction, suggesting that they function in the same developmental network. To test whether *eta1* may be involved in this network, we generated double mutants with *eta1-R* and *lg1-R* or *lg2-219*.

A synergistic interaction was seen between *lg1-R* and *eta1-R* (Figure 4). The *lg1-R eta1-R* homozygotes show a marked displacement of the blade/sheath boundary, which is more severe than the displacement seen with either of the single mutants (Figure 4D). In addition, *eta1-R* homozygotes form ligule tissue and *lg1-R* homozygotes form a rudimentary ligule, but the double mutant fails to form ligule or auricle. Unusual protrusions of undifferentiated tissue were observed on the abaxial leaf surface of double-mutant individuals (Figure 4E, arrows), which are not seen in either *lg1-R* or *eta1-R*

FIGURE 3.—The *eta1-R* mutant displays background effects. (A) Leaf 10 in an *eta1-R*-segregating family in the W23 background, wild type on the left and *eta1* on the right. Note displacement of the blade/sheath boundary and auricle extension (arrows). (B) Leaf 10 in an *eta1-R*-segregating family in the B73 background, wild type on the left and *eta1* on the right. Note reduction of auricle extension (arrows) but blade/sheath boundary remains displaced.

TABLE 3

Effect of genetic background on *eta1* plant height

Background	*n*	Height[a] (SD)	% wild type
B73			
wt	30	191 (±23)	
eta1	11	93 (±15)	49
Mo17			
wt	29	197 (±14)	
eta1	11	117 (±10)	59
W23			
wt	30	193 (±16)	
eta1	14	98 (±12)	51
A188			
wt	13	175 (±10)	
eta1	4	98 (±7)	56

[a] All height measurements are in centimeters and were taken at time of anthesis from the base of the plant to the tip of the tassel.

single mutants. These protrusions did not coincide with venation and were localized to the proximal blade region in the presumptive auricle domain. The novel phenotype of *lg1-R eta1-R* double mutants suggests that these two genes interact synergistically and not additively.

A synergistic interaction was also observed with *lg2-219* and *eta1-R*, but surprisingly, our double-mutant analysis uncovered a dominant dosage effect of the *eta1-R* allele (Figure 5). In the upper adult leaves of the *lg2-219* mutants, ligule and auricle recover. However, *lg2-219* homozygotes that were heterozygous for *eta1-R* displayed extension of auricle in the upper adult leaves (Figure 5C). This dominant dosage effect was confirmed both genetically and molecularly. No notable phenotypic dosage effect was seen with *eta1-R* homozygotes carrying a single copy of the *lg2-219* allele (data not shown). Plants homozygous for both *lg2-219* and *eta1-R* were extremely short, twisted, and often infertile (Figure 5F). The blade/sheath boundary of double-mutant individuals was extremely displaced toward the distal portion of the leaf compared to either of the single mutants, but ligule outgrowth was still apparent. Taken together, the synergistic interaction of *lg1-R* and *eta1-R* and the synergistic dominant dosage effect of *eta1-R* with *lg2-219* place *eta1* in the *liguleless1/2* network of function.

***eta1* enhances regional identity phenotypes:** The *eta1* mutant phenotype is remarkably similar to that of proximodistal regional identity mutants, which cause disruption of the blade/sheath boundary and formation of proximal structures more distally. Of the regional identity mutants, we tested the interaction of *eta1-R* with two of the semidominant class 1 *knox* mutants, *Kn1-N* and *Lg3-O*. To simplify the analysis, only one dose of *Kn1-N* and *Lg3-O* was used. The *eta1-R* mutant enhanced the *Kn1-N* phenotype (Figure 6). Individuals homozygous for *eta1-R* and heterozygous for *Kn1-N* displayed an increase in the number and size of knots, an increase in prominent venation, and an increase in ectopic patches of ligule compared to heterozygous *Kn1-N* siblings (compare Figure 6B with 6D). There is no increase in auricle extension or in displacement of the blade/sheath boundary in the *Kn1-N/+ eta1-R* mutant individuals, suggesting that *eta1-R* is enhancing the *Kn1-N* phenotype.

Similarly, *eta1-R* enhances the *Lg3-O* mutant phenotype (Figure 7). Individuals homozygous for *eta1-R* and heterozygous for *Lg3-O* phenocopied *Lg3-O* homozygotes. Again, there was no significant increase in the amount of auricle tissue in double-mutant individuals, but the leaves were severely proximalized. Double-mutant phenotypes included severe displacement of the blade/sheath boundary, ectopic ligule along the midrib, twisting of the midrib, and alteration in leaf attitude (Figure 7, D and E).

We also tested the interaction of *eta1* with a fully dominant class I *knox* gene, *Gnarley1* (FOSTER *et al.* 1999). *eta1-R* shows a dosage effect with *Gn1-R* as seen in Figure 8. Plants homozygous for *eta1-R* with one copy of *Gn1-R* display an increase in leaf width, an increase in extension of auricle tissue into blade along the margin, and an increase in auricle proliferation at the blade/sheath boundary (compare Figure 8C with 8D).

FIGURE 4.—Synergistic interaction of *lg1-R* and *eta1-R* in the Mo17 background. Adaxial views of leaf 10: (A) wild type, (B) *eta1-R/eta1-R*, (C) *lg1-R/lg1-R*, and (D) *eta1-R/eta1-R lg1-R/lg1-R*. Note the increased displacement of the ligule/auricle line in the double mutant *vs.* that in either of the single mutants (solid arrows). (E) *lg1-R/lg1-R eta1-R/ eta1-R* individual. Open arrows point to ectopic protrusions on the adaxial leaf surface just distal to the blade/sheath boundary.

In families segregating *Gn1-R* alone, *Gn1-R* homozygotes are indistinguishable from heterozygotes (FOSTER *et al.* 1999). However, when a second dose of *Gn1-R* is added in families segregating for *eta1-R*, the phenotype is severely enhanced (Figure 8, E and F). The blade/sheath boundary is severely distorted and the width of blade and sheath is increased. In addition, the leaf is increasingly proximalized with increasing dosage of *Gn1-R*, as sheath and auricle are displaced distally into blade, especially in the region flanking the midrib (Figure 8F). In other words, the *eta1-R* background permits a *Gn1-R* dosage effect that is not evident in a wild-type background.

Both *rs2-R* and *Rs1-O* show a strong synergistic interaction with *eta1-R* (Figure 9). RS2 has homology to MYB-like transcription factors and RS1 is a class 1 *knox* transcription factor. One of the functions of RS2 is to downregulate RS1 in the leaves (SCHNEEBERGER *et al.* 1998). When combined with *eta1-R*, *rs2-R* shows a synergistic interaction such that the *eta1-R* phenotype is exacerbated as well as the *rs2-R* phenotype (Figure 9). The double-mutant individuals show a reduction in height, excessively rough sheath, reduction in sheath length, increased auricle extension, and an overall increase in the proximalization of the leaf compared to *eta1-R* and *rs2-R* single-mutant siblings (compare Figure 9B and 9C with 9D). However, the synergistic interaction of *Rs1-O* and *eta1-R* is subtly different. The overall plant height of *Rs1-O eta1-R* double-mutant individuals is greatly reduced and the sheath length is reduced as is seen with the *rs2-R eta1-R* double mutants. The focus of the ectopic *knox* gene action is shifted distally so that the phenotype is most severe at the auricle region, and the sheath is not particularly rough compared to the *Rs1-O* single

FIGURE 5.—Dosage effect of *lg2-219* and *eta1-R*. Adaxial view of leaf 12 in a *lg2-219 eta1-R*-segregating family in the Mo17/W23 background. (A) Wild type; (B) *lg2-219/lg2-219*; (C) *lg2-219/lg2-219 eta1-R/+*; (D) *eta1-R/eta1-R*; (E) *lg2-219/lg2-219 eta1-R/eta1-R*; (F) whole-plant view of the *lg2-219/lg2-219 eta1-R/eta1-R* double mutant. Arrows mark the auricle extension.

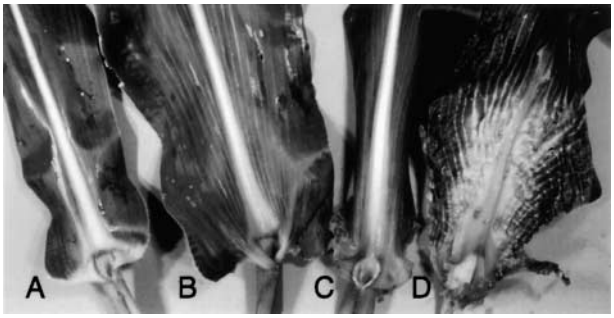

FIGURE 6.—*eta1-R* enhances *Kn1-N*. Adaxial view of leaf 12 from a *Kn1-N/+ eta1-R*-segregating family in the W22 background is shown. This family resulted from an outcross of a plant heterozygous for both *Kn1-N* and *eta1-R* to an individual homozygous for *eta1-R*. (A) Wild type; (B) *Kn1-N/+*; (C) *eta1-R/eta1-R*; (D) *Kn1-N/+ eta1-R/eta1-R*.

mutant. In addition, *Rs1-O eta1-R* double-mutant individuals do not show any ligule outgrowth, are increasingly proximalized with auricle extension flanking the margin, and have very prominent venation in the extended blade/sheath boundary region.

Molecular analyses

***eta1* does not affect *lg1* or *lg2* expression:** To test whether or not *eta1* functions to regulate *lg1* or *lg2* gene expression, we used RT-PCR to analyze expression of LG1- and LG2-mRNA in a family segregating for *eta1-R*. Previous studies have shown that LG2-mRNA expression precedes LG1-mRNA and can be detected in p1–5 leaves (WALSH *et al.* 1998), whereas LG1 is not expressed in early p1–5 leaf primordia but can be seen only in p6–8 leaves (WALSH *et al.* 1998). We isolated mRNA from either meristem and p1–5 or p6–8 leaf primordia and then subjected it to RT-PCR with *lg1*- and *lg2*-specific primers. No difference in mRNA expression of either LG2 or LG1 was found in leaves of *eta1-R* mutants *vs.* their wild-type siblings (Figure 10A). On the basis of these data, *eta1* is not likely to function upstream of *lg1* or *lg2*.

Leaves of *eta1* mutant plants do not ectopically express *knox* genes: The phenotype of *eta1* mutants resembles a number of maize mutants where the molecular cause of the mutant phenotype is ectopic expression of *knox* genes. Because of this, KNOX-mRNA expression was assayed via RT-PCR with primers specific for *lg3, lg4a, lg4b, rs1, gn1,* or *kn1*. No notable differences were seen in *eta1* individuals *vs.* their wild-type siblings with any of these probes. For example, KN1-mRNA expression was detected in meristems of both wild-type and *eta1* mutant individuals, but not in developing leaves (Figure 10B). The same expression pattern was seen with RS1 and GN1 (data not shown). Even after 30 cycles of PCR, we detected no ectopic KN1, GN1, or RS1 expression in *eta1* or wild-type developing leaves (data not shown). LG3-mRNA expression was detected at high levels in meristems and at low levels in developing leaves of wild-type and *eta1* mutant individuals (Figure 10B). Both LG4A and LG4B were expressed in the same pattern as LG3 (data not shown). These results suggest that *eta1* may act downstream of the ectopic *knox* pathway since it does not cause ectopic *knox* gene expression.

Northern blot analysis: The severity of the *Kn1* pheno-

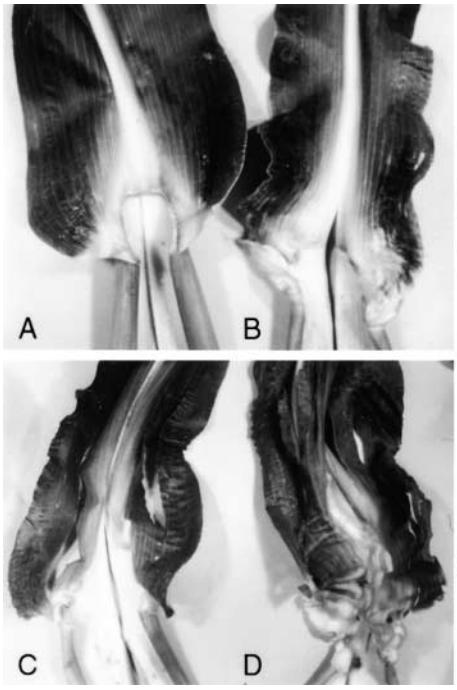

FIGURE 7.—*eta1-R* enhances *Lg3-O*. Adaxial view of leaf 12 from a family segregating *Lg3-O/+ eta1-R* in the Mo17 background is shown. This family resulted from the outcross of a plant heterozygous for both *Lg3-O* and *eta1-R* to a plant homozygous for *eta1-R*. (A) Wild type; (B) *eta1-R/eta1-R*; (C) *Lg3-O/+*; (D) *Lg3-O/+ eta1-R/eta1-R*; (E) mature *Lg3-O/+ eta1-R/eta1-R* plant. Note the severe twisting of the midrib and the change in leaf attitude.

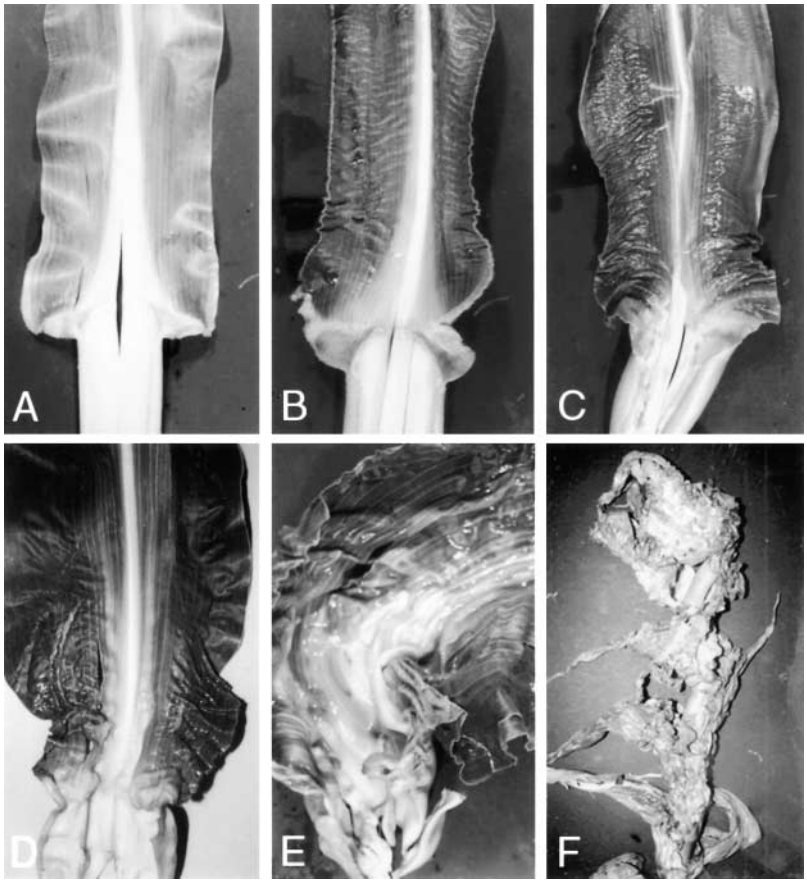

FIGURE 8.—The *eta1-R* mutation shows a dosage effect with *Gn1-R*. Adaxial view of adult leaves from a family segregating *eta1-R Gn1-R* in the W22 background is shown. This family resulted from self-pollination of a plant heterozygous for both *Gn1-R* and *eta1-R*. (A) Wild type; (B) *eta1-R/eta1-R*; (C) *Gn1-R/+*; (D) *Gn1-R/+ eta1-R/eta1-R*; (E) *Gn1-R/Gn1-R eta1-R/eta1-R*; (F) whole-plant view of a *Gn1-R/Gn1-R eta1-R/eta1-R* individual.

type has been correlated with increased KN1-mRNA expression in the leaves (SMITH *et al.* 1992). We wanted to determine if the severe *Kn1-N eta1-R* double-mutant phenotype could be attributed to increased KN1-mRNA levels or if mRNA levels were unchanged. KN1-mRNA is abundant and is easily visualized using Northern blot analysis, which is optimal for direct comparison of RNA concentrations. Figure 10C shows the results of a Northern blot analysis with a *Kn1-N eta1-R*-segregating family in the W22 background. No KN1-mRNA can be detected in *eta1-R* mutant leaves, which is consistent with our RT-PCR findings. Levels of KN1-mRNA did not differ significantly between *Kn1-N/+* and *Kn1-N/+ eta1-R/eta1-R* leaves (lane 4 *vs.* 8). These results further suggest that *eta1* functions downstream of the ectopic *knox* pathway.

DISCUSSION

Much effort in recent years has focused on identifying novel loci in the developmental genetic network controlling proximodistal patterning in the maize leaf. We describe a recessive mutation of the *eta1* gene, *eta1-R*, which affects proximodistal patterning in the maize leaf. To date there are only two published recessive mutations in maize, *rs2* and *sem1*, that are implicated in proximodistal patterning in the leaf and both act to repress *knox* genes (TIMMERMANS *et al.* 1999; TSIANTIS *et al.* 1999; SCANLON *et al.* 2002). While *eta1* is involved in proximodistal patterning in the leaf, *eta1* is unique in that it is not involved in regulating *knox* gene expression. In addition, *eta1* enhances the phenotypes of all known mutants affecting proximodistal patterning in the maize leaf. Thus, our findings implicate *eta1* as a novel and essential component of the developmental genetic network controlling maize leaf development.

The nature of the *eta1-R* mutation and background effects: Genetic evidence from B-A translocations reported here suggests that the *eta1-R* allele is a complete loss-of-function mutation. This amorphy is essential when inferring a functional role for *eta1*. The effect of background on the *eta1* phenotype is not surprising given that background effects are well documented in maize. However, it is intriguing that *eta1-R* displays background expressivities similar to *Lg3-O* (POETHIG 1988; FOWLER and FREELING 1996), being most severe in Mo17 and least severe in B73. This could indicate that similar modifiers are involved in either enhancing or suppressing the aspects of proximodistal patterning in leaf development controlled by *eta1* and disrupted by *Lg3*.

Interaction with the *liguleless* pathway: Previous work with *lg1* and *lg2* suggests that this phenotype is saturated. For example, 18 independent *lg1* alleles and 9 independent *lg2* alleles have been identified, some in genetic

Figure 9.—The *eta1-R* mutation interacts synergistically with *rs2-R* and *Rs1-O*. (A–D) Abaxial view of leaf 12 from a family segregating *rs2-R eta1-R* in the Mo17 background. This family resulted from a self-pollination of an individual heterozygous for both *rs2-R* and *eta1-R*. (A) Wild type; (B) *eta1-R/eta1-R*; (C) *rs2-R/rs2-R*; (D) *rs2-R/rs2-R eta1-R/eta1-R*. (E–H) Abaxial view of leaf 12 from a family segregating *Rs1-O* and *eta1-R* in the Mo17 background. (E) Wild type; (F) *eta1-R/eta1-R*; (G) *Rs1-O/Rs1-O*; (H) *Rs1-O/Rs1-O eta1-R/eta1-R*.

screens to identify other genes in the *liguleless* pathway, but no novel genes have been discovered (D. Braun and J. Walsh, personal communication). It was proposed that other factors in the *liguleless* pathway would be either pleiotropic or lethal (Harper and Freeling 1996a). On the basis of genetic interactions of *eta1* with *lg1* and *lg2* and the *eta1* phenotype, *eta1* can be considered a pleiotropic factor in the *liguleless* network of function. However, given the pleiotropic nature of *eta1*, it is unlikely *eta1* is exclusively functioning in this pathway. RT-PCR gel blot analyses show *eta1* does not affect *lg1* or *lg2* expression. However, *eta1* may act on *lg1* and/or *lg2* at the protein level or perhaps could affect the spatial distribution of LG-mRNAs, which is difficult to test given that the expression patterns of *lg1* and *lg2* have not been precisely discerned. It is likely that *eta1* function is necessary along with *lg1* and *lg2* during early leaf development for correct formation and differentiation of the blade/sheath boundary. *lg1* function seems to be specific to ligule and auricle induction while *lg2* function is specific to regional organ transitions (Walsh and Freeling 1999). *lg2* is involved in early establishment of the blade/sheath boundary during early vegetative stages and in the transition from vegetative to floral branching in the apical tassel meristem (Walsh and Freeling 1999).

Consequently, the synergistic interaction of *eta1* with *lg1* indicates that *eta1* plays a role in the formation of the blade/sheath boundary and in the elaboration of the ligule. Notably, the *lg1* single mutant fails to develop ligule and auricle in the lower leaves but a rudimentary ligule is formed in upper leaves. In contrast, the *eta1 lg1* double mutants do not form rudimentary ligule and the blade/sheath boundary is displaced over the midrib (Figure 4D). This double-mutant phenotype indicates *eta1* is involved in formation of the rudimentary ligule in the absence of *lg1*. This is similar to the dosage-dependent synergistic interaction seen between *lg1* and *lg2*. Double mutants of dominant *Lg3* and *Lg4* alleles with *lg1* and *lg2* also fail to form a rudimentary ligule, but do not enhance the ectopic *knox* phenotypes (Fowler and Freeling 1996). Plants homozygous for

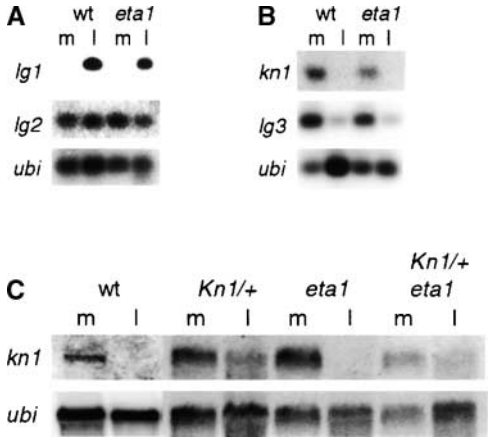

FIGURE 10.—(A) RT-PCR gel blot analysis of LG1 and LG2 expression in an *eta1-R*-segregating family. Lane 1, wild-type meristems and p1–5 leaves; lane 2, wild-type p6–8 leaves; lane 3, *eta1-R* meristems and p1–5 leaves; lane 4, *eta1-R* p6–8 leaves. *Ubiquitin* was used as a loading control. (B) RT-PCR gel blot analysis of *kn1* and *lg3* in an *eta1-R*-segregating family. Lane 1, wild-type meristems and p1–5 leaves; lane 2, wild-type p6–8 leaves; lane 3, *eta1-R* meristems and p1–5 leaves; lane 4, *eta1-R* p6–8 leaves. *Ubiquitin* was used as a loading control. (C) Northern blot analysis of a *Kn1-N/+ eta1/eta1*-segregating family. Lane 1, wild-type meristems and p1–5 leaves; lane 2, wild-type p6–8 leaves; lane 3, *Kn1* meristems and p1–5 leaves; lane 4, *Kn1* p6–8 leaves; lane 5, *eta1* meristems and p1–5 leaves; lane 6, *eta1* p6–8 leaves; lane 7, *eta1 Kn1* meristems and p1–5 leaves; lane 8, *eta1 Kn1* p6–8 leaves. Lanes 1 and 2 are from a different Northern blot than lanes 3–8; however, they represent RNA from the same *Kn1-N eta1-R*-segregating family.

lg1-R and heterozygous and/or homozygous for *lg2-R* failed to form the rudimentary ligule and had a displaced blade/sheath boundary (HARPER and FREELING 1996a). These data indicate *eta1* functions in the same genetic network as *lg1*.

In addition to *lg1* interactions, *eta1* has a directional dosage-dependent interaction with *lg2*. The *eta1-R* allele behaves dominantly to extend auricle tissue in the upper leaves of *lg2-219* homozygous plants. The *lg2 eta1* double mutants also showed extreme displacement of the blade/sheath boundary relative to *eta1* and *lg2* homozygotes. The observation that the double-mutant plants were able to produce ligule suggests that neither of these genes is specifically involved in ligule induction, but may be involved prior to that in establishment of the blade/sheath boundary. These data indicate that *lg2* and *eta1* have partially overlapping functions in properly delineating the blade/sheath boundary.

Interaction with proximodistal axis regional identity mutants: While the mutant *eta1* phenotype resembles that of *rs2* and the dominant *knox* mutants, we found that the *eta1* mutation does not ectopically express any of the class 1 *knox* genes (Figure 10). However, proximodistal regional identity mutants including class 1 *knox* genes interact genetically with *eta1*. Interactions between the dominant *knox* mutants have been previously documented (FOWLER and FREELING 1996). Interestingly, *eta1* can phenocopy dominant *knox* mutations in double-mutant combination. For example, the double-mutant phenotype of *Lg3-O eta1-R* (Figure 7) is nearly identical to the double-mutant phenotype of *Lg3-O Lg4-O* (FOWLER and FREELING 1996). This is also true of the *Kn1-N eta1-R* (Figure 6) double-mutant phenotype, which mimics that of *Kn1-O Rs1-O* (FOWLER and FREELING 1996). Since the severity of *Kn1-N eta1-R* double-mutant individuals is not a direct result of increased KN1-mRNA levels and *eta1-R* in double-mutant combination with *knox* genes results in severe phenotypes, *eta1-R* likely functions either downstream of the pathway perturbed by *knox* neomorphs or in a parallel but convergent pathway that promotes differentiation.

In the *Rs1-O* mutant, the area of ectopic RS1-mRNA expression is greater than one would expect given the phenotypic consequences of that expression (SCHNEEBERGER *et al.* 1995). Specifically, ectopic RS1-mRNA expression can be detected in most cell types but only the sheath and the ligular region display developmental defects. The authors propose that this could be due to competency of cells to respond to ectopic RS1 expression. Perhaps *eta1* is essential in competency and without its normal function cells are increasingly sensitive or responsive to ectopic *knox* gene expression. This could be one explanation for the change in focus of ectopic RS1 action in the *Rs1-O eta1-R* double mutants.

Interestingly, the phenotype of *rs2-R eta1-R* double mutants is slightly different from that of the *Rs1-O eta1-R* double mutants. Both double-mutant analyses were carried out in the same genetic background, which cannot account for the differences observed. It is possible that the difference in the synergistic interaction of *rs2-R eta1-R* compared to *Rs1-O eta1-R* can be attributed to as yet unidentified downstream *rs2* targets, which are likely to be misexpressed. In addition, the spatial and temporal expression of *knox* genes is likely to differ in *Rs1-O* and *rs2-R*. For example, in Arabidopsis, the rounded-leaf phenotype of *as1* mutants differs from that of the lobed-leaf phenotype of *35S:KNAT1* plants (ORI *et al.* 2000; THEODORIS *et al.* 2003).

More surprising is the *eta1 Gn1* dosage effect. *Gn1-R* acts as a true dominant and therefore *Gn1* heterozygotes cannot be distinguished from homozygotes. *rs1* and *gn1* are duplicate genes (FOSTER *et al.* 1999); therefore, it is interesting that we see a dosage effect only with *Gn1-R* and *eta1-R* and not with *Rs1-O* and *eta1-R*. There are multiple explanations for this. One possibility is that the dosage interaction with *eta1-R* and *Gn1-R* is due to allelic differences between *Gn1-R* and *Rs1-O*. Another possibility is that there is a modifier in W22 that confers dosage sensitivity with *Gn1-R eta1-R* and this modifier is not present in Mo17, the background in which the *Rs1-O eta1-R* double-mutant analysis was performed. A third possibility is that although *Rs1* and *Gn1* are thought to be duplicate genes, over evolutionary time they have

evolved slightly disparate functions and thus we found proximodistal identity to be more sensitive to dosage of *Gn1* when *Eta1+* function is lost. These data uncover a threshold of responsiveness to ectopic GN1 that is seen when *Eta1+* function is lost, which is consistent with *eta1* playing a role in competency.

Alternative modes of *eta1* action: Our current understanding of genetic control of patterning in simple leaves comes primarily from work with maize, Antirrhinum, and Arabidopsis. Although there is no precedent in maize for the breadth of interaction seen between *eta1* and the *lg* and *knox* pathways, there is a clue from Arabidopsis on how *eta1* may be functioning. The *pickle* (*pkl*) mutant, which encodes a chromatin-remodeling factor, enhances the *as1* mutant phenotype, but does not ectopically express *knox* genes on its own (Ori *et al.* 2000). These authors propose that *PKL* functions to limit accessibility of *KNOX* genes to their gene targets, while *as1* confers specificity for repression of the *KNOX* genes (Ori *et al.* 2000). Interestingly, the phenotype of *pkl as1* double mutants mimics that of *35S:KNAT1* overexpression lines (Ori *et al.* 2000), much like *eta1* in double-mutant combination with *knox* genes mimics dominant *knox* double mutants. Ori *et al.* (2000) propose that PKL may play a role in restricting competency of cells to respond to morphogenetic factors. Given the pleiotropic phenotype of *eta1* and its many genetic interactors, it is possible *eta1* may have a general function in altering chromatin states and therefore competency similar to *pkl*.

An alternative possibility is that *eta1* functions simply in restricting cell proliferation at the blade/sheath boundary. This seems unlikely given the effects of *eta1* in double-mutant combination with the *knox* genes and *liguleless* genes. Since *lg2* and *Gn1* share only a defect in proper initiation of the blade/sheath boundary, it is more likely that *eta1* functions in establishment of the blade/sheath boundary given its dosage interactions with both *lg2* and *Gn1* (Figures 5 and 8). We have shown that the increase in auricle tissue at the blade/sheath boundary is not solely due to an increase in cell expansion because the auricle cells in *eta1* leaves are similar in size to auricle cells of wild-type siblings (Figure 2, G and H). Another possibility is that *eta1* acts as a receptor or in the reception end of the pathway that establishes the blade/sheath boundary. Further research is focused on the cloning of newly derived *eta1* alleles in hopes of shedding some light on its complex series of genetic interactions. Regardless, *eta1* proves to be an essential component in the genetic circuitry involved with proximodistal patterning in the maize leaf.

Many thanks go to Sarah Hake for alleles, probes, and helpful comments; to Frank Baker for providing the marked B-A translocation stocks; to Randall Tyers for design of the *knox* primers; and to George Theodoris, Randall Tyers, Frank Baker, Noriko Inada, and Nick Kaplinsky for critical reading of the manuscript. Many thanks also go to all of the Freeling lab members past and present who have provided support and guidance in this research, which was supported by National Institutes of Health grant 5R01 GM42610 to M.F.

LITERATURE CITED

Beckett, J. B., 1994a Comprehensive list of B-A translocations in maize, pp. 336–341 in *The Maize Handbook*, edited by M. Freeling and V. Walbot. Springer-Verlag, New York/Berlin.

Beckett, J. B., 1994b Locating recessive genes to chromosome arm with B-A translocations, pp. 315–327 in *The Maize Handbook*, edited by M. Freeling and V. Walbot. Springer-Verlag, New York/Berlin.

Becraft, P. W., and M. Freeling, 1994 Genetic analysis of rough sheath1 developmental mutants of maize. Genetics **136:** 295–311.

Becraft, P. W., D. K. Bongard-Pierce, A. W. Sylvester, R. S. Poethig and M. Freeling, 1990 The liguleless-1 gene acts tissue specifically in maize leaf development. Dev. Biol. **141:** 220–232.

Bellaoui, M., M. S. Pidkowich, A. Samach, K. Kushalappa, S. E. Kohalmi *et al.*, 2001 The Arabidopsis BELL1 and KNOX TALE homeodomain proteins interact through a domain conserved between plants and animals. Plant Cell **13:** 2455–2470.

Byrne, M. E., R. Barley, M. Curtis, J. M. Arroyo, M. Dunham *et al.*, 2000 Asymmetric leaves1 mediates leaf patterning and stem cell function in Arabidopsis. Nature **408:** 967–971.

Byrne, M. E., J. Simorowski and R. A. Martienssen, 2002 ASYMMETRIC LEAVES1 reveals knox gene redundancy in Arabidopsis. Development **129:** 1957–1965.

Edwards, K., C. Johnstone and C. Thompson, 1991 A simple and rapid method for the preparation of plant genomic DNA for Pcr analysis. Nucleic Acids Res. **19:** 1349.

Foster, T., J. Yamaguchi, B. C. Wong, B. Veit and S. Hake, 1999 Gnarley1 is a dominant mutation in the knox4 homeobox gene affecting cell shape and identity. Plant Cell **11:** 1239–1252.

Fowler, J. E., and M. Freeling, 1996 Genetic analysis of mutations that alter cell fates in maize leaves: dominant liguleless mutations. Dev. Genet. **18:** 198–222.

Freeling, M., 1992 A conceptual framework for maize leaf development. Dev. Biol. **153:** 44–58.

Freeling, M., and S. Hake, 1985 Developmental genetics of mutants that specify knotted leaves in maize. Genetics **111:** 617–634.

Hake, S., E. Vollbrecht and M. Freeling, 1989 Cloning knotted the dominant morphological mutant in maize using Ds2 as a transposon tag. EMBO J. **8:** 15–22.

Harper, L., and M. Freeling, 1996a Interactions of liguleless1 and liguleless2 function during ligule induction in maize. Genetics **144:** 1871–1882.

Harper, L., and M. Freeling, 1996b Studies on early leaf development. Curr. Opin. Biotechnol. **7:** 139–144.

Hay, A., H. Kaur, A. Phillips, P. Hedden, S. Hake *et al.*, 2002 The gibberellin pathway mediates KNOTTED1-type homeobox function in plants with different body plans. Curr. Biol. **12:** 1557–1565.

Kerstetter, R. A., D. Laudencia-Chingcuanco, L. G. Smith and S. Hake, 1997 Loss-of-function mutations in the maize homeobox gene, knotted1, are defective in shoot meristem maintenance. Development **124:** 3045–3054.

Li, Y., G. Hagen and T. J. Guilfoyle, 1992 Altered morphology in transgenic tobacco plants that overproduce cytokinins in specific tissues and organs. Dev. Biol. **153:** 386–395.

Long, J. A., E. I. Moan, J. I. Medford and M. K. Barton, 1996 A member of the KNOTTED class of homeodomain proteins encoded by the STM gene of Arabidopsis. Nature **379:** 66–69.

Moreno, M. A., L. C. Harper, R. W. Krueger, S. L. Dellaporta and M. Freeling, 1997 Liguleless1 encodes a nuclear-localized protein required for induction of ligules and auricles during maize leaf organogenesis. Genes Dev. **11:** 616–628.

Muehlbauer, G. J., J. E. Fowler and M. Freeling, 1997 Sectors expressing the homeobox gene liguleless3 implicate a time-dependent mechanism for cell fate acquisition along the proximal-distal axis of the maize leaf. Development **124:** 5097–5106.

Mueller, J., Y. Wang, R. Franzen, L. Santi, F. Salamini *et al.*, 2001 In vitro interactions between barley TALE homeodomain proteins suggest a role for protein-protein associations in the regulation of Knox gene function. Plant J. **27:** 13–23.

Ori, N., M. T. Juarez, D. Jackson, J. Yamaguchi, G. M. Banowetz *et*

al., 1999 Leaf senescence is delayed in tobacco plants expressing the maize homeobox gene knotted1 under the control of a senescence-activated promoter. Plant Cell **11:** 1073–1080.

Ori, N., Y. Eshed, G. Chuck, J. L. Bowman and S. Hake, 2000 Mechanisms that control knox gene expression in the Arabidopsis shoot. Development **127:** 5523–5532.

Poethig, R. S., 1988 Heterochronic mutations affecting shoot development in maize. Genetics **119:** 959–974.

Poethig, S., 1984 Cellular parameters of leaf morphogenesis in maize Zea-mays and tobacco Nicotiana-tabacum, pp. 235–260 in *Contemporary Problems in Plant Anatomy; Symposium, Chapel Hill, North Carolina*, edited by R. A. White and W. C. Dickison. Academic Press, Orlando, FL/London.

Sakamoto, T., N. Kamiya, M. Ueguchi-Tanaka, S. Iwahori and M. Matsuoka, 2001 KNOX homeodomain protein directly suppresses the expression of a gibberellin biosynthetic gene in the tobacco shoot apical meristem. Genes Dev. **15:** 581–590.

Scanlon, M. J., R. G. Schneeberger and M. Freeling, 1996 The maize mutant narrow sheath fails to establish leaf margin identity in a meristematic domain. Development **122:** 1683–1691.

Scanlon, M. J., D. C. Henderson and B. Bernstein, 2002 SEMAPHORE1 functions during the regulation of ancestrally duplicated knox genes and polar auxin transport in maize. Development **129:** 2663–2673.

Schneeberger, R. G., P. W. Becraft, S. Hake and M. Freeling, 1995 Ectopic expression of the knox homeo box gene rough sheath1 alters cell fate in the maize leaf. Genes Dev. **9:** 2292–2304.

Schneeberger, R., M. Tsiantis, M. Freeling and J. A. Langdale, 1998 The rough sheath2 gene negatively regulates homeobox gene expression during maize leaf development. Development **125:** 2857–2865.

Smith, L. G., B. Greene, B. Veit and S. Hake, 1992 A dominant mutation in the maize homeobox gene, Knotted-1, causes its ectopic expression in leaf cells with altered fates. Development **116:** 21–30.

Smith, J. S. C., E. C. L. Chin, H. Shu, O. S. Smith, S. J. Wall *et al.*, 1997 An evaluation of the utility of SSR loci as molecular markers in maize (Zea may L.): comparisons with data from RFLPS and pedigree. Theor. Appl. Genet. **95:** 163–173.

Smith, H. M. S., I. Boschke and S. Hake, 2002 Selective interaction of plant homeodomain proteins mediates high DNA-binding affinity. Proc. Natl. Acad. Sci. USA **99:** 9579–9584.

Steeves, T. A., and I. M. Sussex, 1989 *Patterns in Plant Development*, Ed. 2. Cambridge University Press, New York/Cambridge, UK.

Sylvester, A. W., W. Z. Cande and M. Freeling, 1990 Division and differentiation during normal and liguleless-1 maize leaf development. Development **110:** 985–1000.

Theodoris, G., N. Inada and M. Freeling, 2003 Conservation and molecular dissection of *ROUGH SHEATH2* and *ASYMMETRIC LEAVES1* function in leaf development. Proc. Natl. Acad. Sci. USA **100:** 6837–6842.

Timmermans, M. C. P., A. Hudson, P. W. Becraft and T. Nelson, 1999 Rough sheath2: a Myb protein that represses knox homeobox genes in maize lateral organ primordia. Science **284:** 151–153.

Tsiantis, M., R. Schneeberger, J. F. Golz, M. Freeling and J. A. Langdale, 1999 The maize rough sheath2 gene and leaf development programs in monocot and dicot plants. Science **284:** 154–156.

Vollbrecht, E., B. Veit, N. Sinha and S. Hake, 1991 The developmental gene knotted-1 is a member of a maize homeobox gene family. Nature **350:** 241–243.

Vollbrecht, E., L. Reiser and S. Hake, 2000 Shoot meristem size is dependent on inbred background and presence of the maize homeobox gene, knotted1. Development **127:** 3161–3172.

Walsh, J., and M. Freeling, 1999 The liguleless2 gene of maize functions during the transition from the vegetative to the reproductive shoot apex. Plant J. **19:** 489–495.

Walsh, J., C. A. Waters and M. Freeling, 1998 The maize gene liguleless 2 encodes a basic leucine zipper protein involved in the establishment of the leaf blade-sheath boundary. Genes Dev. **12:** 208–218.

Communicating editor: J. Birchler